

$N\Omega$ dibaryon from lattice QCD near the physical point

Takumi Iritani^a, Sinya Aoki^b, Takumi Doi^{a,c}, Faisal Etminan^d,
Shinya Gongyo^a, Tetsuo Hatsuda^{c,a}, Yoichi Ikeda^e, Takashi Inoue^f,
Noriyoshi Ishii^e, Takaya Miyamoto^b, Kenji Sasaki^b, (HAL QCD
Collaboration)

^a*RIKEN Nishina Center (RNC), Saitama 351-0198, Japan*

^b*Yukawa Institute of Theoretical Physics, Kyoto Univ., Kyoto 606-8502, Japan*

^c*RIKEN Interdisciplinary Theoretical and Mathematical Sciences Program (iTHEMS),
Saitama 351-0198, Japan*

^d*Dept. of Phys., Faculty of Sciences, University of Birjand, Birjand 97175-615, Iran*

^e*Research Center for Nuclear Physics (RCNP), Osaka Univ., Osaka 567-0047, Japan*

^f*College of Bioresource Science, Nihon Univ., Kanagawa 252-0880, Japan*

Abstract

The nucleon(N)-Omega(Ω) system in the S-wave and spin-2 channel (5S_2) is studied from the (2+1)-flavor lattice QCD with nearly physical quark masses ($m_\pi \simeq 146$ MeV and $m_K \simeq 525$ MeV). The time-dependent HAL QCD method is employed to convert the lattice QCD data of the two-baryon correlation function to the baryon-baryon potential and eventually to the scattering observables. The $N\Omega({}^5S_2)$ potential, obtained under the assumption that its couplings to the D-wave octet-baryon pairs are small, is found to be attractive in all distances and to produce a quasi-bound state near unitarity: In this channel, the scattering length, the effective range and the binding energy from QCD alone read $a_0 = 5.30(0.44)({}^{+0.16}_{-0.01})$ fm, $r_{\text{eff}} = 1.26(0.01)({}^{+0.02}_{-0.01})$ fm, $B = 1.54(0.30)({}^{+0.04}_{-0.10})$ MeV, respectively. Including the extra Coulomb attraction, the binding energy of $p\Omega^-({}^5S_2)$ becomes $B_{p\Omega^-} = 2.46(0.34)({}^{+0.04}_{-0.11})$ MeV. Such a spin-2 $p\Omega^-$ state could be searched through two-particle correlations in p - p , p -nucleus and nucleus-nucleus collisions.

Keywords: dibaryon, Lattice QCD, hyperon interaction

Email address: takumi.iritani@riken.jp (Takumi Iritani)

1. Introduction

Quest for dibaryons is a long-standing experimental and theoretical challenge in hadron physics [1, 2]. Among various theoretical attempts to study dibaryons, one of the recent highlights is the (2+1)-flavor lattice QCD simulations near the physical point ($m_\pi \simeq 146$ MeV and $m_K \simeq 525$ MeV) by HAL QCD Collaboration. (For a recent summary, see Ref.[3].) This enables us to make model-independent investigations of the elusive H -dibaryon, originally proposed by the MIT bag model [4], on the basis of a coupled channel analysis of the lattice QCD data [5]. Also, the possible di-Omega ($\Omega\Omega$), originally proposed by the Skyrme model [6], has recently been examined in detail from the same lattice QCD data [7].

Another interesting candidate of the dibaryon is $N\Omega$ ($uudsss$ or $uddsss$) in the 5S_2 channel. Since the Pauli exclusion does not operate among valence quarks and the color-magnetic interaction is attractive in the channel, it was predicted to be a resonance below the $N\Omega$ threshold in the constituent quark model [8, 9]. Moreover, $N\Omega({}^5S_2)$ is expected to have relatively a small width since its strong decay into octet baryons such as $\Lambda\Xi$ and $\Sigma\Xi$, which must have orbital D-wave, would be kinematically suppressed. A pilot (2+1)-flavor lattice QCD simulations with a heavy pion mass ($m_\pi \simeq 875$ MeV) [10] suggests a short-range attraction between N and Ω in the 5S_2 channel. Subsequently, theoretical studies on the $N\Omega$ system [11, 12, 13, 14, 15] as well as experimental measurements in relativistic heavy ion collisions [16] have been reported.

The purpose of this Letter is to study $N\Omega({}^5S_2)$ on the basis of realistic (2+1)-flavor lattice QCD simulations near the physical point ($m_\pi \simeq 146$ MeV and $m_K \simeq 525$ MeV). As in the case of our previous pilot study [10], we employ the HAL QCD method [17, 18, 19] which allows us to extract the interaction between N and Ω from the spacetime dependence of the two-baryon correlation function on the lattice.

This paper is organized as follows. In Sec. 2, we introduce the HAL QCD method to extract the hadron interaction from lattice QCD. In Sec. 3, we summarize the setup of our lattice QCD simulations near the physical point. In Sec. 4, we analyze the $N\Omega$ system in 5S_2 channel in detail. Sec. 5 is devoted to summary and concluding remarks.

2. HAL QCD method

Let us consider the $N\Omega(^5S_2)$ characterized by the following two-baryon correlation function,

$$C_{N\Omega}(\vec{r}, t) = \frac{1}{24} \sum_{\mathcal{R} \in \mathcal{O}} \sum_{\vec{x}} P_{\alpha\beta, \ell; \alpha'\beta', \ell'}^{(s=2)} \langle 0 | N_\alpha(\mathcal{R}[\vec{r}] + \vec{x}, t) \Omega_{\beta, \ell}(\vec{x}, t) \overline{\mathcal{J}}_{\alpha'\beta', \ell'}^{N\Omega}(0) | 0 \rangle, \quad (1)$$

with $\mathcal{J}^{N\Omega}$ being the wall-type quark source. The interpolating operators for the nucleon and the Ω -baryon are

$$N_\alpha(x) = \varepsilon_{abc} (u^{aT}(x) C \gamma_5 d^b(x)) q_\alpha^c(x), \quad \Omega_{\beta, \ell}(x) = \varepsilon_{abc} s_\beta^a(x) (s^{bT}(x) C \gamma_\ell s^c(x)), \quad (2)$$

where α and β are Dirac indices, ℓ is a spatial label of gamma matrices, a , b , c are the color indices and $C \equiv \gamma_4 \gamma_2$ and Dirac indices are restricted to the upper two components. The summation over the cubic group element $\mathcal{R} \in \mathcal{O}$ leads to a projection onto the S-wave state¹. On the other hand, the projection operator onto the spin-2 state $P_{\alpha\beta, \ell; \alpha'\beta', \ell'}^{(s=2)}$ picks the diagonal elements of S_z for the source and the sink and takes the average of $S_z = \pm 2, \pm 1, 0$ states, which corresponds to $E^+ \oplus T_2^+$ irreducible representations of $SO(3, \mathbf{Z})$ [20, 21].

In the present paper, we assume that the couplings of $N\Omega(^5S_2)$ to the D-wave octet-octet channels *below* the $N\Omega$ threshold ($\Lambda\Xi$ and $\Sigma\Xi$) are small.² If this holds true, the t -dependence of the correlation function $C_{N\Omega}(\vec{r}, t)$ would be dominated by $N\Omega(^5S_2)$ for certain range of t before the octet-octet channels take over at large t . We also assume that the coupling to the inelastic octet-decuplet channels (such as $\Lambda\Xi^*$ located just *above* the $N\Omega$ threshold) is sufficiently small in the range of t adopted in the present paper.³ If such inelastic contributions are not negligible, not only the t -dependence but also

¹Strictly speaking, this operation projects onto the A_1^+ state which contains not only $L = 0$ state but also $L = 4, 6, \dots$ states in the continuum theory.

²A recent phenomenological study indicates that the volume integral of the $N\Omega(^5S_2)$ potential from the D-wave octet-octet channels below the $N\Omega$ threshold are insignificant $\sim 10\%$ (Table IV of [14]).

³The contributions from the $N\Omega(^5D_2)$, $N\Omega(^3D_2)$ and $\Lambda\Xi^*(^5S_2)$ to the volume integral of the $N\Omega(^5S_2)$ potential are found to be negligible $\sim \mathcal{O}(1)\%$ in a phenomenological study (Table IV of [14]).

the non-locality of the single-channel $N\Omega(^5S_2)$ potential would become significant. To check the effects of the neglected states mentioned above in more detail, the coupled-channel analysis of the HAL QCD method [22] is necessary. We leave it as a future problem.

To extract the single-channel $N\Omega(^5S_2)$ potential, it is convenient to define the following ratio which we call the “ R -correlator”,

$$R_{N\Omega}(\vec{r}, t) \equiv \frac{C_{N\Omega}(\vec{r}, t)}{C_N(t)C_\Omega(t)}, \quad (3)$$

where $C_N(t)$ and $C_\Omega(t)$ are single-baryon correlators. Below the inelastic threshold, $R_{N\Omega}(\vec{r}, t)$ can be shown to satisfy the integro-differential equation with a non-local and energy-independent kernel $U(\vec{r}, \vec{r}')$ [19],

$$\left[-\frac{\partial}{\partial t} + \frac{1 + 3\delta^2}{8m} \frac{\partial^2}{\partial t^2} + \mathcal{O}(\delta^2\partial_t^3) \right] R(\vec{r}, t) = H_0 R(\vec{r}, t) + \int U(\vec{r}, \vec{r}') R(\vec{r}', t) d\vec{r}', \quad (4)$$

with $H_0 \equiv -\nabla^2/2m$, the reduced mass $m \equiv (m_N m_\Omega)/(m_N + m_\Omega)$ and the asymmetry parameter $\delta \equiv (m_N - m_\Omega)/(m_N + m_\Omega)$.

The central potential in the leading-order (LO) analysis under the derivative expansion $U(\vec{r}, \vec{r}') = \sum_n V_n(\vec{r}) \nabla^n \delta(\vec{r} - \vec{r}')$ is given by⁴

$$V_C(r) = -\frac{H_0 R_{N\Omega}(\vec{r}, t)}{R_{N\Omega}(\vec{r}, t)} - \frac{(\partial/\partial t) R_{N\Omega}(\vec{r}, t)}{R_{N\Omega}(\vec{r}, t)} + \frac{1 + 3\delta^2}{8m} \frac{(\partial^2/\partial t^2) R_{N\Omega}(\vec{r}, t)}{R_{N\Omega}(\vec{r}, t)}, \quad (5)$$

up to $\mathcal{O}(\delta^2\partial_t^3)$ -terms in the right hand side. Spatial and temporal derivatives on the lattice at (\vec{r}, t) are calculated in central difference scheme using nearest neighbour points. If $R_{N\Omega}(\vec{r}, t)$ is dominated by a single state at large t , each term in the r.h.s. of Eq. (5) should have no t -dependence. Such a single-state saturation, however, is not necessary to obtain $V_C(r)$ in the time-dependent HAL QCD method as long as $R_{N\Omega}(\vec{r}, t)$ is dominated by the elastic states. In general, each term in the r.h.s. receives t -dependence which provides

⁴Good convergence of this derivative expansion at low energies for the point-sink scheme has been demonstrated [23, 24] for the NN and $\Xi\Xi$ channels where the long-range part of the potentials are expected to be dominated by the single-pion exchange. Such a good convergence in other channels without one-pion exchange such as $N\Omega$ and $\Omega\Omega$ needs to be checked explicitly in the future.

“signal” instead of “noise” for $V_C(r)$. (If there remains residual t -dependence in $V_C(r)$, it implies the necessity of the next-to-leading order of the derivative expansion and/or the channel coupling to other states [23, 24].) This is why the data at moderate values of $t \sim 1$ fm are sufficient to extract the baryon-baryon interaction in HAL QCD method.⁵

3. Lattice Setup

Gauge configurations are generated by using the (2+1)-flavor lattice QCD with the Iwasaki gauge action at $\beta = 1.82$ and the non-perturbatively $\mathcal{O}(a)$ -improved Wilson quark action with the six APE stout smearing with the smearing parameter $\rho = 0.1$ at nearly physical quark masses ($m_\pi \simeq 146$ MeV and $m_K \simeq 525$ MeV) [31]. The lattice cutoff is $a^{-1} \simeq 2.333$ GeV ($a \simeq 0.0846$ fm) and the lattice volume L^4 is 96^4 , corresponding to $La \simeq 8.1$ fm. This is sufficiently large volume to accommodate two baryons. We employ the wall-type quark source with the Coulomb gauge fixing. The periodic (Dirichlet) boundary condition for the spatial (temporal) direction is imposed for quarks. The quark propagators are obtained by using the domain-decomposed solver [32, 33, 34, 35], and the unified contraction algorithm is employed to calculate the correlation functions [36].

The forward and backward propagations are averaged and the hypercubic symmetry on the lattice (4 rotations) are utilized for each configuration. 414 configurations are available by picking up one per five trajectories: For 207 configurations which are separated by ten trajectories, 48 source locations are used, while 24 source locations are used for the rest (207 configurations), and the total number of measurements read 119,232. The statistical errors are estimated by the jackknife method with 20 samples (bin size 5,952 measurements). We have checked that the bin size dependence is small by comparing the result with 40 samples (bin size 2,880 measurements). The fit to the effective mass in the range $12 \leq t/a \leq 17$ for N and $17 \leq t/a \leq 22$ for Ω lead to $m_N = 954.7(2.7)$ MeV and $m_\Omega = 1711.5(1.0)$ MeV. These values

⁵This is in sharp contrast to the so-called “finite volume method” for two-baryon systems. It requires strict ground state saturation, so that very large value of $t > 10$ fm is necessary. For such large t , however, no signal can be obtained due to the explosion of statistical errors. See [25, 26, 27, 28] for explicit demonstration of this fact. Note also that this problem has been recognized in the studies of meson-meson scatterings [29] and the use of the variational method [30] is known to be mandatory.

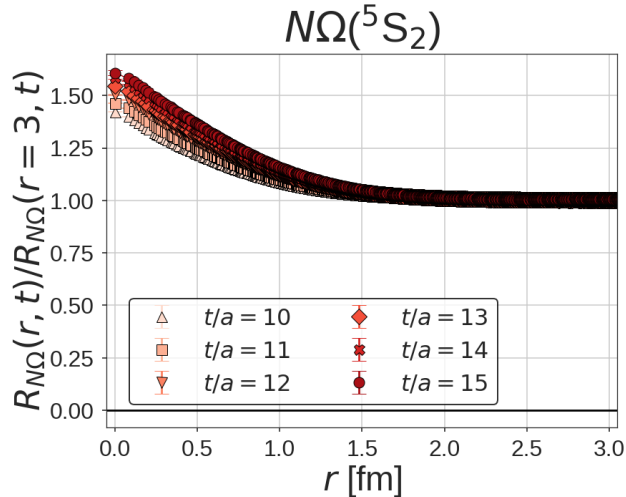


Figure 1: The rescaled R -correlator of the $N\Omega(^5S_2)$ in the range $t/a = 10 - 15$.

are about 2% heavier than physical values due to a slight difference of the present quark masses from the physical point.

4. Spin-2 $N\Omega$ potential

Shown in Fig. 1 is the R -correlator defined by Eq. (3) in the range $t/a = 10 - 15$, which are rescaled by the value of $r = 3$ fm. At large r , the R -correlator approaches a constant. This implies that $V_C(r)$ in Eq. (5) becomes a constant at long distance. At small r , the R -correlator increases with the second-order derivative in r being always positive, which implies that there is an attractive potential at short distances. The weak t -dependence at small r indicates contributions from the elastic scattering states. As mentioned before, this t -dependence provides signal instead of noise.

To extract $V_C(r)$ from the R -correlator, we choose $t/a = 11 - 14$ in order to reduce the systematic uncertainties⁶: For smaller values of t , the inelastic contribution starts to appear so that $V_C(r)$ remains non-vanishing even for large r . For larger values of t , it is difficult to control the systematic uncertainties of the fitting of the potential due to the large statistical errors. Note

⁶Due to the presence of time derivatives up to $\mathcal{O}(\partial_t^2)$, the actual lattice data used in our analysis are in the interval $10 \leq t/a \leq 15$.

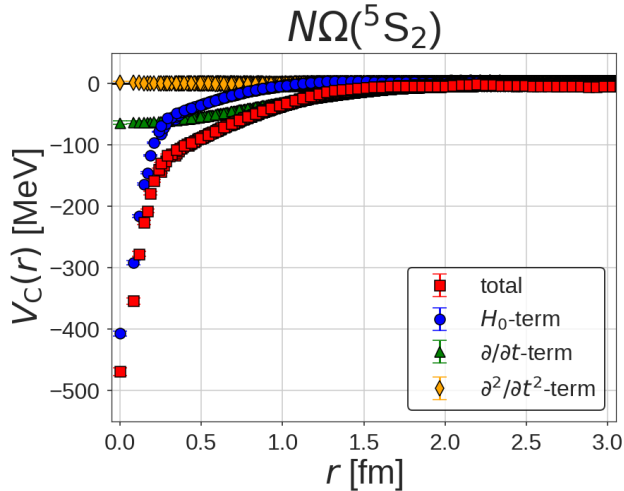


Figure 2: The central potential (red squares) at $t/a = 12$ and its breakdown into the H_0 -term (blue circles), the $\partial/\partial t$ -term (green triangles) and the $\partial^2/\partial t^2$ -term (orange diamonds).

that we take relatively larger values of t/a to make accurate determination of m_N and m_Ω , whose values agree with the effective masses at $t/a = 12$ in 1%.

In Fig. 2, $V_C(r)$ as well as its breakdown into different components are shown for $t/a = 12$ as an example. First of all, $V_C(r)$ (red squares) is attractive everywhere. This is qualitatively consistent with the result in our pilot study with heavy pion mass ($m_\pi \simeq 875$ MeV) [10]. Also, we found that the H_0 -term (blue circles) is dominant, yet the $\partial/\partial t$ -term (green triangles) gives non-negligible r -dependent contribution. On the other hand, the $\partial^2/\partial t^2$ -term (orange diamonds) is consistent with zero.

We summarize the central potential $V_C(r)$ in Fig. 3(a) for $t/a = 11 - 14$. These potentials are consistent with each other within statistical errors, which is a necessary (but not sufficient) condition for the small coupling with the D-wave octet-octet states below the $N\Omega$ threshold in the spin-2 channel. (Such a stability of the potential in the same range of t in the spin-1 $N\Omega$ system is not found, which indicates the strong coupling of the $N\Omega(^3S_1)$ state to the S-wave octet-octet states below threshold.) In the followings, we estimate the corresponding systematic errors as well as errors from the truncation of the derivative expansion and from the contamination of the inelastic states by utilizing the time dependence of the results.

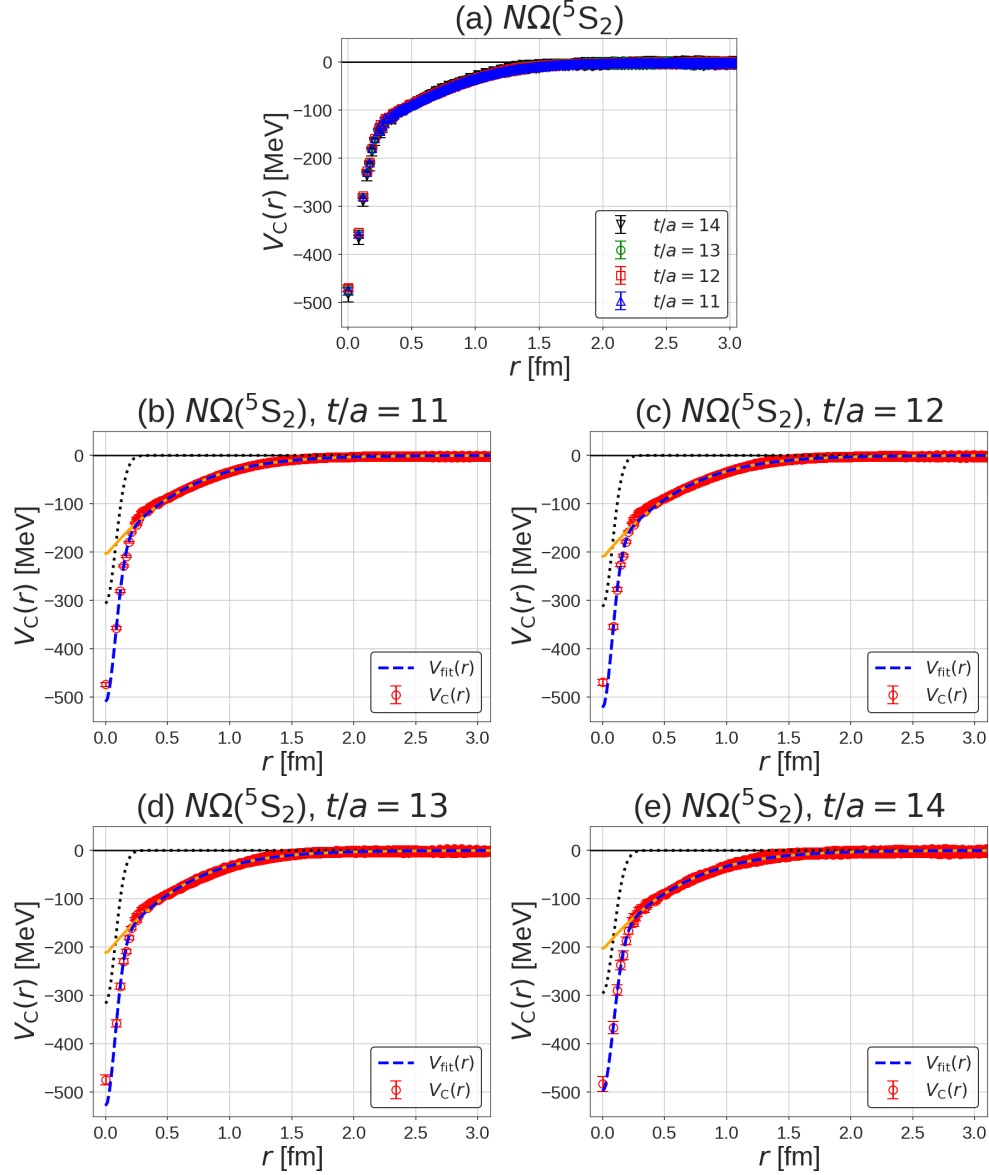


Figure 3: (a) The central potential $V_C(r)$ of the $N\Omega(^5S_2)$ system at $t/a = 11$ (blue up-pointing triangles), 12 (red squares), 13 (green circles) and 14 (black down-pointing triangles). (b) The result of the fitting of $V_C(r)$ (red circles) at $t/a = 11$ by using $V_{\text{fit}}(r)$ in Eq. (6). The black dotted (orange solid) line denotes the first (second) term in Eq. (6), and the blue dashed line is the sum of two terms. (c), (d) and (e) are the cases of $t/a = 12$, 13 and 14, respectively.

To obtain observables such as the scattering phase shifts and binding energy, we fit the lattice QCD potential by Gaussian + (Yukawa)² with a form factor [10]:

$$V_{\text{fit}}(r) = b_1 e^{-b_2 r^2} + b_3 \left(1 - e^{-b_4 r^2}\right)^n \left(\frac{e^{-m_\pi r}}{r}\right)^2. \quad (6)$$

The (Yukawa)² form at long distance is motivated by the picture of two-pion exchange between N and Ω with an OZI violating vertex [14]. The pion mass in Eq. (6) is taken from our simulation, $m_\pi = 146$ MeV, and we fit the data at $r < 3$ fm. After trying both $n = 1$ and 2 in the form factor, we found that only $n = 1$ can reproduce the short distance behavior of the lattice potential, so that we will focus on the $n = 1$ case below. The results of the fit and the corresponding parameters are summarized in Fig. 3(b,c,d,e) and Table 1, respectively⁷.

t/a	11	12	13	14
b_1 [MeV]	-306.5(5.5)	-313.0(5.3)	-316.7(9.4)	-296(18)
b_2 [fm ⁻²]	73.9(4.4)	81.7(5.4)	81.9(8.4)	64(16)
b_3 [MeV·fm ²]	-266(32)	-252(27)	-237(43)	-272(109)
b_4 [fm ⁻²]	0.78(11)	0.85(10)	0.91(18)	0.76(34)

Table 1: The fitting parameters in Eq. (6) in physical unit with the statistical errors.

Shown in Fig. 4 (Left) is the S-wave scattering phase shift δ_0 as a function of the kinetic energy. The values of $k \cot \delta_0$ are also shown in Fig. 4 (Right). These results for $t/a = 11, 12, 13$ and 14 are consistent with each other within the statistical errors. In the $k \rightarrow 0$ limit, the phase shift approaches to 180° , and the scattering length,⁸ $a_0 \equiv -\lim_{k \rightarrow 0} \tan \delta_0/k$, becomes positive. This implies the existence of a quasi-bound state of $N\Omega$ in the 5S_2 channel.

The effective range expansion (ERE) of the phase shifts up to the next-

⁷ In order to examine the fit range dependence, we compare the fit with the data in $r < 2.5$ fm and that in $r < 3$ fm by using the functional form of Eq. (6). The resultant scattering parameters are found to be consistent with each other within statistical errors. In addition, results for another functional form with three Gaussian are found to be consistent with those obtained from Eq. (6) within the statistical errors.

⁸Here, the sign of the scattering length is defined to be opposite to that in [10].

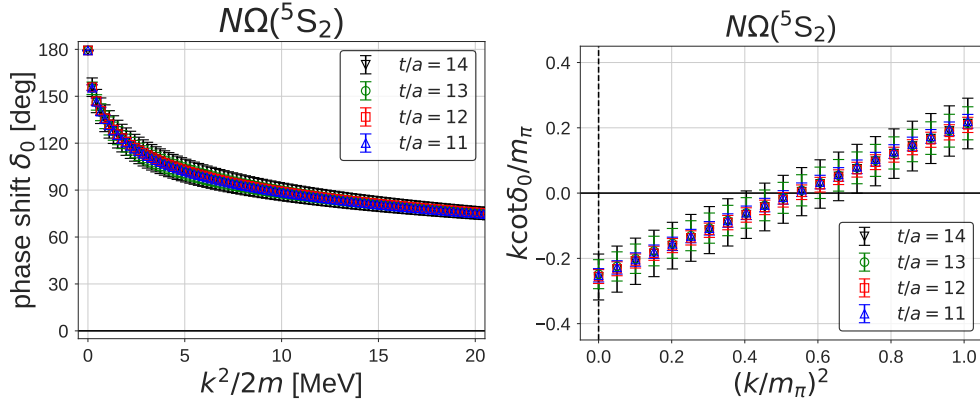


Figure 4: (Left) The S-wave scattering phase shifts δ_0 as a function of the kinetic energy, $k^2/2m$. (Right) $k \cot \delta_0/m_\pi$ as a function of $(k/m_\pi)^2$.

leading-order (NLO) reads

$$k \cot \delta_0 = -\frac{1}{a_0} + \frac{1}{2}r_{\text{eff}}k^2 + O(k^4) \quad (7)$$

with r_{eff} being the effective range. The ERE parameters (a_0, r_{eff}) obtained from our phase shifts are found to be

$$a_0 = 5.30(0.44)({}^{+0.16}_{-0.01}) \text{ fm}, \quad r_{\text{eff}} = 1.26(0.01)({}^{+0.02}_{-0.01}) \text{ fm}, \quad (8)$$

where the central values and the statistical errors are estimated at $t/a = 12$, while the systematic errors in the last parentheses are estimated from the central values for $t/a = 11, 13$ and 14 .

In Fig. 5, the ratio r_{eff}/a_0 as a function of r_{eff} for $N\Omega(^5S_2)$ is plotted together with the experimental values for $NN(^3S_1)$ (deuteron) and $NN(^1S_0)$ (di-neutron) as well as lattice QCD value for $\Omega\Omega(^1S_0)$ (di-Omega) [7]. Small values of $|r_{\text{eff}}/a_0|$ in all these cases indicate that these systems are located close to the unitary limit.⁹

The binding energy B and the root mean square distance ($\sqrt{\langle r^2 \rangle}$) of $N\Omega(^5S_2)$ are obtained by solving the Schrödinger equation with the potential

⁹The values in the fm unit are $(a_0, r_{\text{eff}})_{NN(^3S_1)} = (5.4112(15), 1.7463(19))$, $(a_0, r_{\text{eff}})_{NN(^1S_0)} = (-23.7148(43), 2.750(18))$ from the experiment [37], and $(a_0, r_{\text{eff}})_{\Omega\Omega(^1S_0)} = (4.6(6)({}^{+1.2}_{-0.5}), 1.27(3)({}^{+0.06}_{-0.03}))$ from the lattice QCD calculation [7].

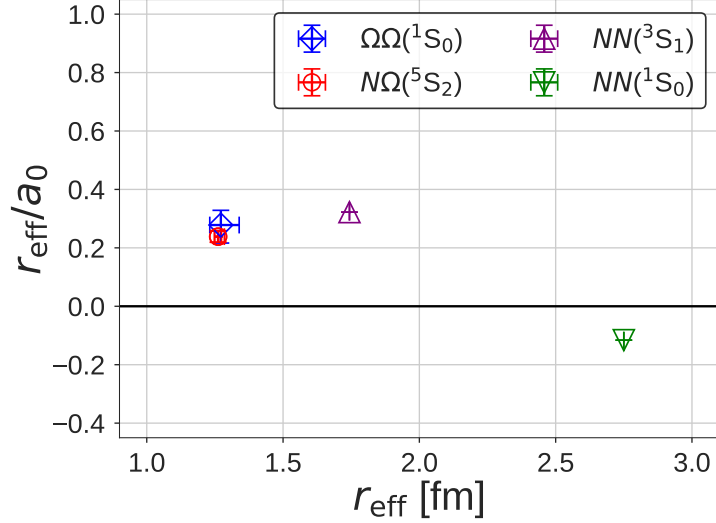


Figure 5: The ratio of the effective range r_{eff} and the scattering length a_0 as a function of r_{eff} for $N\Omega(^5S_2)$ (red circle) and $\Omega\Omega(^1S_0)$ [7] (blue diamond) on the lattice, as well as for $NN(^3S_1)$ (purple up-pointing triangle) and $NN(^1S_0)$ (green down-pointing triangle) [37] in experiments.

fitted to our lattice results:

$$B = 1.54(0.30)_{(-0.10)}^{(+0.04)} \text{ MeV}, \quad \sqrt{\langle r^2 \rangle} = 3.77(0.31)_{(-0.01)}^{(+0.11)} \text{ fm}. \quad (9)$$

Although the N - Ω is attractive everywhere, the binding energy is as small as ~ 1 MeV due to the short range nature of the potential. Accordingly, the root mean square distance is comparable to the scattering length, indicating that the system is loosely bound like the deuteron and the di-Omega.

In our pilot study [10], we found $B = 18.9(5.0)_{(-1.8)}^{(+12.1)}$ MeV for heavy pion mass $m_\pi = 875$ MeV. The larger magnitude of B than the present result in Eq. (9) originates partly from the heavy masses of N and Ω in [10] which reduce the kinetic energy and thus increase the binding energy. Another reason is that the short-range attraction for heavy pion is relatively stronger.

So far, we have not considered extra attraction in the $p\Omega^-$ system due to Coulomb attraction. By taking into account the correction $V_C(r) \rightarrow V_C(r) - \alpha/r$ with $\alpha \equiv e^2/(4\pi) = 1/137.036$, we obtain the observables,

$$B_{p\Omega^-} = 2.46(0.34)_{(-0.11)}^{(+0.04)} \text{ MeV}, \quad \sqrt{\langle r^2 \rangle}_{p\Omega^-} = 3.24(0.19)_{(-0.00)}^{(+0.06)} \text{ fm}. \quad (10)$$

These results for $p\Omega^- (^5S_2)$ are summarized in Fig. 6 together with $n\Omega^- (^5S_2)$ without Coulomb correction.

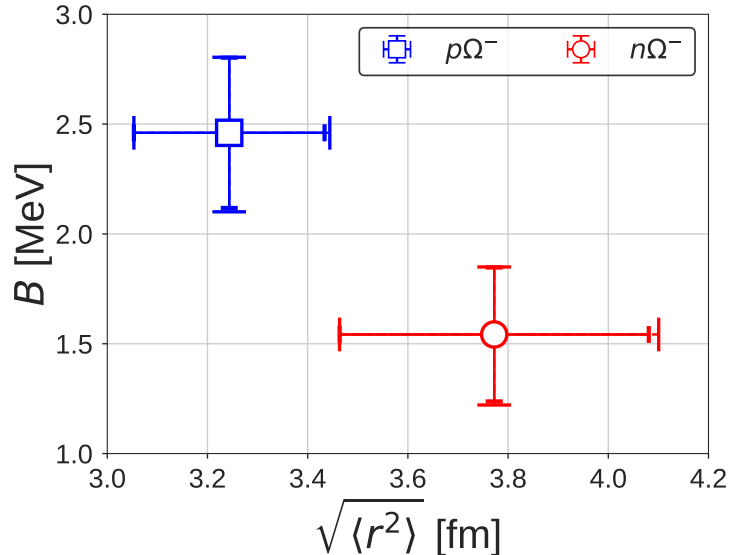


Figure 6: The binding energy B and the root mean square distance $\sqrt{\langle r^2 \rangle}$ for $n\Omega^-$ (red circle) and for $p\Omega^-$ (blue square). In both figures, inner bars correspond to the statistical errors, while the outer bars are obtained by the quadrature of the statistical and systematic errors.

Before ending this section, let us briefly discuss other possible systematic errors in Eqs. (8), (9) and (10). The first one is the finite volume effect whose typical error would be $\exp(-2m_\pi(L/2)) \simeq \exp(-6) \simeq 0.25\%$ and is much smaller than the statistical errors in our simulation. The second one is the finite cutoff effect, which is also expected to be small assuming the naive order estimate $(\Lambda a)^2 \leq 1\%$ with the non-perturbative $\mathcal{O}(a)$ improvement. The third systematic error is due to the slightly heavy hadron masses ($m_\pi = 146$ MeV, $m_N = 955$ MeV and $m_\Omega = 1712$ MeV). By using the same parameter set for $t/a = 12$ in Table 1 with $m_\pi = 146$ MeV kept fixed but with physical baryon masses ($m_p = 938$ MeV and $m_{\Omega^-} = 1672$ MeV), we find less binding than Eq. (10) as expected: $B_{p\Omega^-} \simeq 2.18(32)$ MeV and $\sqrt{\langle r^2 \rangle}_{p\Omega^-} \simeq 3.45(22)$ fm. On the other hand, if we additionally employ $m_\pi^\pm = 140$ MeV for the potential (see Eq. (6)), we find more bounding than Eq. (10) due to smaller pion mass: $B_{p\Omega^-} \simeq 3.00(39)$ MeV and $\sqrt{\langle r^2 \rangle}_{p\Omega^-} \simeq 3.01(16)$ fm.

5. Summary

In this paper, we have studied the N - Ω system in the 5S_2 channel, which is one of the promising candidates for quasi-stable dibaryon, from the (2+1)-flavor lattice QCD simulations with nearly physical quark masses ($m_\pi \simeq 146$ MeV and $m_K \simeq 525$ MeV). The N - Ω central potential in the 5S_2 channel obtained by the time-dependent HAL QCD method is found to be attractive in all distances. The scattering length and the effective range obtained by solving the Schrödinger equation using the resultant potential show that $N\Omega({}^5S_2)$ is close to unitarity similar to the cases of the deuteron (pn) and di-Omega ($\Omega\Omega$). The binding energy of $p\Omega^-$ without (with) the Coulomb attraction is about 1.5 MeV (2.5 MeV), which indicates the existence of a shallow quasi-bound state below the $N\Omega$ threshold. In our simulation, we did not find a signature of the strong coupling between $N\Omega({}^5S_2)$ and $\Lambda\Xi$ or $\Sigma\Xi$ in the D-wave state, while it remains to be an important future problem to analyze the coupled channel system with octet baryons, $\Lambda\Xi$ and $\Sigma\Xi$.

The $N\Omega({}^5S_2)$ in the unitary regime can be studied in the two-particle correlation measurements in p - p and p -nucleus and nucleus-nucleus collisions as suggested theoretically in [12] and experimentally reported by the STAR Collaboration at RHIC [16]. Phenomenological analyses along this line on the basis of the results in the present paper will be reported elsewhere [38].

Acknowledgements

We thank members of PACS Collaboration for the gauge configuration generation. The lattice QCD calculations have been performed on the K computer at RIKEN (hp120281, hp130023, hp140209, hp150223, hp150262, hp160211, hp170230), HOKUSAI FX100 computer at RIKEN (G15023, G16030, G17002) and HA-PACS at University of Tsukuba (14a-20, 15a-30). We thank ILDG/JLDG [39, 40] which serves as an essential infrastructure in this study. We thank the authors of cuLGT code [41] for the gauge fixing. This research was supported by SPIRE (Strategic Program for Innovative REsearch), MEXT as “Priority Issue on Post-K computer” (Elucidation of the Fundamental Laws and Evolution of the Universe) and JICFuS. This work is supported by JSPS Grant-in-Aid for Scientific Research, No. 18H05236, 18H05407, 16H03978, 15K17667. T.H. is grateful to the Aspen Center for Physics, supported in part by NSF Grants PHY1607611. The authors thank T. Sekihara, K. Morita, and A. Ohnishi for fruitful discussions, and H. Nemura and Y. Namekawa for useful comments.

References

- [1] H. Clement, *Prog. Part. Nucl. Phys.* **93**, 195 (2017) [arXiv:1610.05591 [nucl-ex]].
- [2] S. Cho *et al.* [ExHIC Collaboration], *Prog. Part. Nucl. Phys.* **95**, 279 (2017) [arXiv:1702.00486 [nucl-th]].
- [3] T. Doi, “Baryon interactions at physical quark masses in Lattice QCD”, talk at Lattice 2018 (East Lansing, USA), July 22-28, 2018. <https://indico.fnal.gov/event/15949/session/13/contribution/92>
- [4] R. L. Jaffe, *Phys. Rev. Lett.* **38**, 195 (1977) Erratum: [ibid. 617 (1977)].
- [5] K. Sasaki *et al.* [HAL QCD Collaboration], *EPJ Web Conf.* **175**, 05010 (2018).
- [6] V. B. Kopeliovich, B. Schwesinger and B. E. Stern, *Phys. Lett. B* **242**, 145 (1990).
- [7] S. Gongyo *et al.*, *Phys. Rev. Lett.* **120**, 212001 (2018) [arXiv:1709.00654 [hep-lat]].
- [8] J. T. Goldman, K. Maltman, G. J. Stephenson, Jr., K. E. Schmidt and F. Wang, *Phys. Rev. Lett.* **59**, 627 (1987).
- [9] M. Oka, *Phys. Rev. D* **38**, 298 (1988).
- [10] F. Etminan *et al.* [HAL QCD Collaboration], *Nucl. Phys. A* **928**, 89 (2014) [arXiv:1403.7284 [hep-lat]].
- [11] H. Huang, J. Ping and F. Wang, *Phys. Rev. C* **92**, 065202 (2015) [arXiv:1507.07124 [hep-ph]].
- [12] K. Morita, A. Ohnishi, F. Etminan and T. Hatsuda, *Phys. Rev. C* **94**, 031901 (2016) [arXiv:1605.06765 [hep-ph]].
- [13] J. Haidenbauer, S. Petschauer, N. Kaiser, U. G. Meissner and W. Weise, *Eur. Phys. J. C* **77**, 760 (2017) [arXiv:1708.08071 [nucl-th]].
- [14] T. Sekihara, Y. Kamiya and T. Hyodo, *Phys. Rev. C* **98**, 015205 (2018) [arXiv:1805.04024 [hep-ph]].

- [15] H. Garcilazo and A. Valcarce, Phys. Rev. C **98**, 024002 (2018) [arXiv:1810.04382 [nucl-th]].
- [16] J. Adam *et al.* [STAR Collaboration], Phys. Lett. **B790**, 490 (2019) arXiv:1808.02511 [hep-ex].
- [17] N. Ishii, S. Aoki and T. Hatsuda, Phys. Rev. Lett. **99**, 022001 (2007) [nucl-th/0611096].
- [18] S. Aoki, T. Hatsuda and N. Ishii, Prog. Theor. Phys. **123**, 89 (2010) [arXiv:0909.5585 [hep-lat]].
- [19] N. Ishii *et al.* [HAL QCD Collaboration], Phys. Lett. **B712**, 437 (2012) [arXiv:1203.3642 [hep-lat]].
- [20] S. Basak *et al.* [Lattice Hadron Physics (LHPC) Collaboration], Phys. Rev. D **72**, 074501 (2005) [hep-lat/0508018].
- [21] J. J. Dudek, R. G. Edwards, M. J. Peardon, D. G. Richards and C. E. Thomas, Phys. Rev. D **82**, 034508 (2010) [arXiv:1004.4930 [hep-ph]].
- [22] S. Aoki, B. Charron, T. Doi, T. Hatsuda, T. Inoue and N. Ishii, Phys. Rev. D **87**, 034512 (2013) [arXiv:1212.4896 [hep-lat]].
- [23] T. Iritani *et al.* [HAL QCD Collaboration], Phys. Rev. D **99**, 014514 (2019) [arXiv:1805.02365 [hep-lat]].
- [24] K. Murano, N. Ishii, S. Aoki and T. Hatsuda, Prog. Theor. Phys. **125**, 1225 (2011) [arXiv:1103.0619 [hep-lat]].
- [25] T. Iritani *et al.*, JHEP **1610**, 101 (2016) [arXiv:1607.06371 [hep-lat]].
- [26] T. Iritani *et al.*, Phys. Rev. D **96**, 034521 (2017) [arXiv:1703.07210 [hep-lat]].
- [27] S. Aoki, T. Doi and T. Iritani, EPJ Web Conf. **175**, 05006 (2018) [arXiv:1707.08800 [hep-lat]].
- [28] T. Iritani *et al.* [HAL QCD Collaboration], JHEP **1903** (2019) 007 [arXiv:1812.08539 [hep-lat]].

- [29] R. A. Briceño, J. J. Dudek and R. D. Young, *Rev. Mod. Phys.* **90**, 025001 (2018) [arXiv:1706.06223 [hep-lat]], and references therein.
- [30] M. Lüscher and U. Wolff, *Nucl. Phys. B* **339**, 222 (1990).
- [31] K.-I. Ishikawa *et al.* [PACS Collaboration], *PoS LATTICE 2015*, 075 (2016) [arXiv:1511.09222 [hep-lat]].
- [32] T. Boku *et al.*, *PoS LATTICE 2012*, 188 (2012) [arXiv:1210.7398 [hep-lat]].
- [33] M. Terai, K. I. Ishikawa, Y. Sugisaki, K. Minami, F. Shoji, Y. Nakamura, Y. Kuramashi, M. Yokokawa, “Performance Tuning of a Lattice QCD code on a node of the K computer,” *IPSJ Transactions on Advanced Computing Systems*, Vol.6 No.3 43-57 (Sep. 2013) (in Japanese).
- [34] Y. Nakamura, K.-I. Ishikawa, Y. Kuramashi, T. Sakurai and H. Tadano, *Comput. Phys. Commun.* **183**, 34 (2012) [arXiv:1104.0737 [hep-lat]].
- [35] Y. Osaki and K. I. Ishikawa, *PoS LATTICE 2010*, 036 (2010) [arXiv:1011.3318 [hep-lat]].
- [36] T. Doi and M. G. Endres, *Comput. Phys. Commun.* **184**, 117 (2013) [arXiv:1205.0585 [hep-lat]].
- [37] R. W. Hackenburg, *Phys. Rev. C* **73**, 044002 (2006).
- [38] K. Morita, S. Gongyo, T. Hatsuda, T. Iritani, A. Ohnishi, and K. Sasaki, in preparation.
- [39] <http://www.lqcd.org/ildg>, <http://www.jldg.org>
- [40] T. Amagasa *et al.*, *J. Phys. Conf. Ser.* **664**, 042058 (2015).
- [41] M. Schröck and H. Vogt, *Comput. Phys. Commun.* **184**, 1907 (2013) [arXiv:1212.5221 [hep-lat]].